Manuscript submitted to: Volume 3, Issue 1, 75-100.

AIMS Energy DOI: 10.3934/energy.2015.1.75

Received date 1 December 2014, Accepted date 29 January 2015, Published date 6 February 2015

Review

Materials for hydrogen storage and the Na-Mg-B-H system

Daphiny Pottmaier [1,2,*] and Marcello Baricco [3]

[1] Innovation Park , The Energy Technologies Building, Jubilee Campus, University of Nottingham, Triumph Road, NG7 2TU Nottingham, United Kingdom
[2] Department of Mechanical Engineering, Federal University of Santa Catarina, Fpolis, Brazil
[3] Dipartimento di Chimica & NIS, Università di Torino, via Pietro Giuria 7/9, I-10125 Turin, Italy

* **Correspondence:** Email: dpottmaier@gmail.com; Tel: +44 (0)115-74-84530; Fax: +44 (0)115-95-13159.

Abstract: This review on materials for hydrogen storage in the solid state gives a brief discussion underlying reasons and driving forces of this specific field of research and development (the why question). This scenario is followed by an outline of the main materials investigated as options for hydrogen storage (the what exactly). Then, it moves into breakthroughs in the specific case of solid state storage of hydrogen, regarding both materials (where to store it) and properties (how it works). Finally, one of early model systems, namely $NaBH_4/MgH_2$ (the case study), is discussed more comprehensively to better elucidate some of the issues and drawbacks of its use in solid state hydrogen storage.

Keywords: complex hydrides; solid-state reactions; hydrogen storage; renewable energy

1. Hydrogen Storage Scenario

Change to a hydrogen-based energy society [1], with its promise of a clean and sustainable choice, is clearly a complex issue involving mainly economic and political drivers. On the one hand, economic and societal issues include energy dependence, costs, global warming, pollution, and safety. On the other hand, political and governmental concerns include insufficient investment in research, inadequate legislation, and development of an infrastructure. These variables are essential at both local and global levels. By the eyes of science and technology, development and implementation of this hydrogen economy may enclose solutions along the hydrogen chain: from production, distribution, storage, utilization, up to its recycling.

Hydrogen is the most attractive energy carrier. It presents the highest heating value (141.8 MJ/kg) among known fuels (diesel 44.8, gasoline: 47.3, methane 55.5); has a non-polluting product

(H_2O) from its process of energy conversion (electrochemical or combustion); it is the most abundant element (75 wt.% of the universe). Moreover, hydrogen is a safe fuel as diffuses (0.61 cm^2/s) thorough air more rapidly than other gaseous fuels, with the highest stoichiometric air/fuel ratio (H_2 34.3 kg, diesel 14.5, gasoline 14.6, methane 17.2), very high auto-ignition temperature (H_2 585 ºC, diesel 180, gasoline 260, methane 540). Naturally, along modern history, generation of energy appears to be moving towards a more efficient fuel with higher hydrogen density [2]:

$$\text{C (COAL)} \rightarrow \text{CH}_2\text{- (OIL)} \rightarrow \text{CH}_4 \text{ (NATURAL GAS)} \rightarrow \text{H}_2 \text{ (HYDROGEN)}$$

However, hydrogen (boiling point −253 ºC) is not present in nature as a single element or in any other state of matter, rather is bounded to other elements as in water and other organic compounds. In general, most of the elements in the periodic table react with hydrogen to form simple or complex hydrides under appropriate conditions (temperature and hydrogen pressure).

Today, hydrogen can be extracted using different processes: from coal gasification, from oil and natural gas from steam reforming, from wood pyrolysis, from ethanol alcoholysis, from algae photosynthesis, and from water electrolysis [3,4]. Thus, hydrogen is only as green as its production method, leading us to the risk of a faulty development of hydrogen and fuel cell technologies without comparable implementation of renewable energy sources. Regarding distribution of hydrogen, this will be apparently less problematic as, like the existent fuels, it is related to production and utilization, which may also profit from present fuel system such as oil tank trucks and natural gas pipelines. Hydrogen is utilized as a fuel in fuel cells, which is an electrochemical device that through the reaction of hydrogen and oxygen produces electricity ($0.40V_{hydrogen} + 0.83V_{oxygen} = 1.23V$), heat and water. Higher voltage are reached by combining fuel cells, each one with two electrodes (anode: oxidation; cathode: reduction) separated by a solid or liquid electrolyte. Types of fuel cell, according to operating temperature and constituent material, can be listed as: alkaline (AFC) [5], proton exchange membrane (PEMFC) [6], molten carbonate (MCFC) [7], and solid oxide (SOFC) [8], with costs and durability as major problems.

Each one of these segments of the hydrogen chain has an important role in achieving the prospective of a hydrogen-based economy. However, a common factor along the chain is the interaction between materials and hydrogen. Thus, materials will play a crucial role regardless its place in this hydrogen era. More importantly, once produced, hydrogen must be stored as a synthetic fuel for generation of energy. So, hydrogen storage is a known bottleneck, from economical to safety concerns.

Hydrogen storage systems comprehend of three main classes, regarding the hydrogen state: high-pressure/gaseous, liquid and solid-state storage. A summary of the present scenario is given herein (Table 1) and the most relevant findings related to these technologies are listed in a report by the International Energy Agency (IEA), as part of the Hydrogen Implementing Agreement (HIA) [9]. The importance of hydrogen was seriously realized as early as 1974, when the International Association for Hydrogen Energy (IAHE) was founded followed in 1977 by the Hydrogen Program, part of the IEA and counting with 21 countries [10]. More recently, from 2006 to 2011, the US-Department of Energy (DOE) decided to advance of hydrogen storage materials and established three Centers of Excellence (CoE): the Metal Hydride (MHCoE) [11], the Chemical Hydride (CHCoE) [12], and the Hydrogen Sorption (HSCoE) [13]. More about the materials being investigated on the three centres can be found in a recently published book [14]. Similar programs are running in Europe, Japan, Korea and other countries.

Table 1. Present scenario of the approaches for hydrogen storage.

	Gas	Liquid	Solid
Status	Commercially available, but costly	Commercially available, but costly	Very early development
Best Option	C-fibre composite vessels (6–10 wt.% at 350–700 atm, ~40 kg/m^3)	Cryogenic insulated dewars (ca. 20 wt.% at −253 °C under 1 atm, ~70 kg/m^3)	Too early to define. Most developed option: metal hydrides (>8 wt.%, >90 kg/m^3, at 10–60 atm)
R&D issues	Fracture mechanics, compression energy, volume reduction, safety.	High liquefaction energy, dormant boil off, safety.	Weight density, working temperatures and pressures, recharge time, heat management, cost, pyrophoricity, cycling.

For commercial applications, according to the ultimate targets proposed by the US-DOE [15], an ideal hydrogen storage system must meet the following minimum criteria:

- high storage capacity (>7.5% kg H_2 /kg, >70 kg H_2 /m^3),
- reasonable charging/discharging rates (<2 kg H_2 /min),
- good operating conditions (<85 ºC, <12 atm H_2),
- high thermal conductivity (dissipation of sorption heat),
- reversibility (1,500 working cycles),
- low cost (<2–3 US$ / kg H_2).

These criteria are mainly based on the performance of synthetic fuels in use today (e.g. diesel, gasoline). Even though there are still research for application of gaseous and liquid hydrogen storage methods, the very low boiling point of hydrogen in the liquid state (−253 ºC) and its low density in the gaseous state (0.126 kg/m^3) make them only temporary solutions due to reasons such as low energy efficiency and users safety, respectively. Solid hydrogen storage may be the most promising method to fulfil the targets. Indeed, IEA points out a more promising scenario for approaches in the solid state from the materials and systems considered for hydrogen storage.

Hydrogen can be stored in the solid state in two modes: ad/physisorption—hydrogen remains in its molecular form interacting with compounds by weak bonds (heat of reaction < 10 kJ/mol); whereas ab/chemisorption—hydrogen in its atomic form reacts with other elements by forming primary bonds (heat of reaction > 50 kJ/mol). An ideal material will have a heat of reaction in the range between 10 and 50 kJ/mol, which then will present the required conditions for hydrogen storage. Reviews on the first class of materials (ad/physorption) can be found elsewhere [16,17,18]. For the second class of materials (ab/chemisorption), main systems under consideration are given in the sequence, others systems and further details can also be found in other relevant reviews [19–22].

2. Milestones in Solid Hydrogen Storage

The most remarkable findings reported in the literature are chronologically described in the sequence: starting with the reversibility with catalysts (M-Al-H system), M = alkali, earth-alkali and transition metal, nanostructuring by ball milling (M-H system), lowering temperatures and pressures with amides (M-N-H system), reaching high hydrogen capacities with borohydrides (M-B-H system), and finally, tailoring thermodynamics with mixed systems (M-H + M-X-H), X = B, Al. Additionally

to these hydride systems, hydrogen can bond differently with the same elements in order to form different compounds (Table 2).

Table 2. Materials for hydrogen storage and periodic table of hydrides.

	Class	System			
Elements	*Alkali Metals*	MH	NaH		
	Alkali Earth-Metals	MH_2	MgH_2		
	Transitions Metals	MH	NiH	; MH_2	TiH_2
Alloys	*Solid Solutions*				
	Intermetallics	MY_5H_6	$LaNi_5H_6$	; M_2YH_4	Fe_2NiH_4
Complexes	*Poor Metals*	$MAlH_4$	$NaAlH_4$		
	Non-Metals	MBH_4	$NaBH_4$	; $M(BH_4)_2$	$Ca(BH_4)_2$
		MNH_2	$LiNH_2$	; M_2NH	Li_2NH
	Mixed	MBH_3NH_3	$LiBH_3NH_3$		
	Others	Polyhydrides		CH_4	

ionic *covalent*

LiH	BeH_2											**BH_3**	CH_4	NH_3	H_2O	HF
NaH	**MgH_2**	*metallic*										AlH_3	SiH_4	PH_3	H_2S	HCl
KH	CaH_2	ScH_2	TiH_2	VH	CrH	MnH	Fe	Co	NiH	CuH	ZnH_2	GaH_3	GeH_4	AsH_3	H_2Se	HBr
RbH	SrH_2	YH_3	ZrH_2	NbH_2	Mo	Tc	Ru	Rh	PdH	AgH	CdH_2	InH_3	SnH_4	SbH_3	H_2Te	HI
CsH	BaH_2		HfH_2	TaH	WH_3	ReH_7	Os	Ir	PtH	AuH_3	HgH_2	TlH_3	PbH_4	BiH_3	Po	At
Fr	Ra															
		LaH_3	CeH_3	PrH_2	NdH	Pm	SmH_2	EuH_2	GdH_2	TbH_2	DyH_2	HoH_2	ErH_2	TmH_2	YbH_3	LuH_2
		AcH_2	ThH_2	PaH_2	UH_3	NpH_2	PuH_2	AmH_2	Cm	Bk	Cf	Es	Fm	Nd	No	Lr

at room temperature: solid, liquid, gaseous, unknown hydride.

As can be observed by the periodic table of hydrides, most elements bond to hydrogen to form hydrides, as solid, liquid or gas phases at room temperature [23]. Binary hydrides (MH_x) show also deviations from stoichiometry (x = 1, 2, 3) and exist as multi-phase systems. Atoms of hydrogen occupy the interstitial sites in the lattice structure of these elements; in the octahedral or tetrahedral interstices, or a combination of the two. Some hydrides are formed under high pressures, e.g. SiH_4 (HCP) > 250 GPa [24], PtH (HCP) > 47 GPa [25]. Actually, all noble metals (Ru, Rh, Pd, Ag, Os, Ir, Pt, Au) [26] and some transition metals (Cr, Mn, Fe, Co, Ni, Mo,W) [27] form hydrides under high pressures. As a remark, it is to remind that most hydrides have high reactivity with air, even at RT, and water. Physically, metallic hydrides are often grey or black powder. Moreover, carbon and hydrogen form a wide range of compounds: ethane (C_2H_6) and other alkanes (simple bond), ethylene (C_2H_4) and other alkenes (double bond), acetylene (C_2H_2) and other alkynes (triple bond), etc. Nitrogen and hydrogen also form another known hydride, called hydrazine (N_2H_4). From the halogen hydrides, boiling points increase as HCl (189 K) < HBr (206 K) < HI (238 K) < HF (292.5 K), thus

only HF is liquid at room temperature (RT).

Among metallic elements, the only one forming hydrides under reasonable range (0–100 ºC, 1–10 atm) is vanadium [28]. Among binary compound of hydrogen, the one with the highest hydrogen content per weight is Methane (CH_4) with 25 wt.%. Other compounds with high content are the gases diborane (B_2H_6) with 22 wt.%, ammonia (NH_3) with 18 wt.% and water, with 11 wt.%.

2.1. Reversibility with catalysts—in the M-Al-H system

In 1997, Bogdanovic et al. have shown in their pioneering work that Ti-doping of pure $NaAlH_4$ (5.6 wt.% H_2) promotes the reversibility of hydrogen release reactions, by enhancing kinetics close to ambient temperature [29]:

$$NaAlH_4 \quad \leftrightarrow \quad 1/3Na_3AlH_6 + 2/3Al + H_2 \leftrightarrow NaH + Al + 3/2H_2 \qquad (1)$$

The reversible absorption—desorption isotherm was shown as the first plateau region at about 180 ºC under 160 bar with small hysteresis. Later in 2000, the same group presented a more detailed work on the Ti-doped $NaAlH_4$, in which measurements were taken under lower temperatures and pressures, so that the system can be considered as a potential hydrogen storage material [30]. Since then, several research groups have been investigating the origin and mechanisms of the Ti-doping effect on the reversibility of this system [31,32,33]. Overall, catalyst doping was found to dramatically improve kinetics. For example, by XRD it was confirmed that $TiCl_3$ reacts with $NaAlH_4$ to form NaCl and that partial desorption of $NaAlH_4$ occurs already during the catalyst doping process by ball milling [34]. Moreover, the catalyst effect in the system is such that a one-step direct synthesis of Ti-doped $NaAlH_4$ from NaH–Al–$TiCl_3$ mixtures under low temperature and pressure conditions, in considerably short reaction time [35]. However, reaction mechanisms in hydrogen sorption reactions were not fully understood yet and there is still an increasing interest of research to significantly enhances kinetics and favours thermodynamics [36]. The use of the M-Al-H system, as well as of a wide range of new catalysts in the system, is one of the main areas inside the investigation of hydrogen storage materials. Indeed, the US-MHCoE has a main arm of research exclusively dedicated to M-Al-H systems, particularly AlH_3 and $LiAlH_4$.

2.2. Nanostructuring by ball milling—of the M-H system

Among all known reversible hydrides, MgH_2 has the highest hydrogen capacity (7.66 wt.%) summing up low equilibrium conditions (at 287 ºC under 1 atm hydrogen) [37]:

$$MgH_2 \leftrightarrow Mg + H_2 \qquad (2)$$

However, sorption reactions are slow and occur at relatively higher temperature than the target for portable applications. The first successful route to overcome these drawbacks was patented in 1999 by Zaluska et al. [38], which introduced nanosizing of materials by ball milling in the hydrogen storage field. It was verified that nanostructuring of MgH_2 by ball milling promotes a change in the morphology of the initial powders [39]. Moreover, this enhances surface activity and consequently sorption kinetics, lowering of operating temperatures, and no need for activation. Nowadays,

ball-milling process is considered a standard in preparing powder materials for hydrogen storage systems and other approaches were introduced such as the reactive mechano-synthesis [40]. More recently, more direct nanoengineering have been introduced into the field as encapsulation of nanoparticles and utilization of nanoscaffolds or nanopores. For example, such nano-approaches have proven to increase performance in some practical requirements (e.g. reaction times, operational temperatures) [41], however, so far at the expense of other characteristics (e.g. thermal conductivity, cyclability). These size effects on the hydrogen storage has been reviewed in detail [42].

2.3. Low temperatures—within the M-N-H systems

In 2002, Chen et al. have reported reversible hydrogen sorption reactions up to 9.3 wt.% in Li_3N, corresponding to 11.5 wt. % theoretical capacity, at 255 ºC in 30 min by the two-step reaction [43]:

$$LiNH_2 + 2LiH \leftrightarrow Li_2NH + H_2 + LiH \leftrightarrow Li_3N + 2H_2 \qquad (3)$$

Actually, hydrogen in non-isothermal conditions starts to react in this system at a temperature as low as 100 ºC. However, hydrogen desorption under vacuum conditions has main release step at 175 ºC and completion was only reached above 400 °C. According to these results, the plateau for 1 atm hydrogen is predicted at 285 °C. Moreover, the reaction mechanism involved in the sorption reactions of $LiNH_2$ is likely to be mediated by ammonia, through a fast reaction between LiH and NH_3 [44]. LiH captures NH_3 gas during the hydrogenation of Li_3N and, therefore, prevents this undesirable gas to escape into the hydrogen stream during the dehydrogenation process [45]. Catalytic effect of $TiCl_3$ was observed to be effective in the transport of NH_3 molecule in the interface LiH-$LiNH_2$, which was confirming the importance of the surface effects in these solid state reactions [46]. Partial oxidation of Li_3N was shown to improve kinetics of hydrogenation-dehydrogenation to a reversible 5.0 wt.% H_2 in only 3 min at 180 °C as a result of a newly formed Li_2O/Li_3N system, which does not decrease its cyclability [47]. Preheating of Li_3N under vacuum at 400 °C was effective in improving hydrogen storage of this Li-N-H system, which was attributed to its relatively large particle sizes. Overall, this is a materials system with inherently fast kinetics, good reversibility and stability, reasons for placing amides/imides as suitable candidates for on-board applications. Thus, it was a notable breakthrough opening investigation of M-N-H systems for hydrogen storage in the solid state.

2.4. High hydrogen capacities—of the M-B-H systems

A year later, in 2003 Zuttel et al. have demonstrated that the decomposition temperature of $LiBH_4$ starting at about 100 °C with SiO_2 catalyst could release up to about 18.5 wt.% hydrogen [48]. Nonetheless, the hydrogen content released was 13.8 wt.% for partial desorption reaction:

$$LiBH_4 \leftrightarrow LiH + B + 3/2H_2 \qquad (4)$$

Pure $LiBH_4$ only starts releasing hydrogen around 300 °C, which is slightly above its melting point (277 °C), meaning that reaction only occurs in the liquid state. Indeed, later it was shown by in-situ measurements that SiO_2 reacts with molten $LiBH_4$ to form Li_2SiO_3 or Li_4SiO_4 and it was also

demonstrated a faster reactivity with the addition of $TiCl_3$, forming LiCl at room temperature [49]. Following the use of SiO_2, other systems were also used to destabilize pure $LiBH_4$, such as oxides [50], halides [51], and rare-earth compounds [52]. Improvement of reaction kinetics was also interestingly demonstrated by addition of pure boron [53,54]. Another method to enhance kinetics is by nanoscaffolding incorporation [55]. In fact, combining Pt nanoparticles as a catalyst [56,57], nanoconfinement of $LiBH_4$ in graphene has showed to improve its de/rehydrogenation, even at very low catalyst content, with a reversible capacity of ca. 8.1 wt.% [58]. Even though, the sorption properties of $LiBH_4$ have been tailored considerably throughout the years with the great efforts of researchers, they remain impractical for portable applications, particularly on-board transport. Nonetheless, introduction of this candidate borohydride, with its high hydrogen capacity, was significant in the development of research on complex hydrides regarding hydrogen storage.

2.5. Thermodynamic tailoring—using mixed (M-H + M-X-H) systems

Later in 2004, Luo et al. and Xiong et al. have proposed a possible destabilization of $LiNH_2$ by partial substitution of Li with Mg [59,60]. They demonstrated experimentally that the $LiNH_2/MgH_2$ system can reach 4.5 wt.% of hydrogen uptake at about 200 °C, suggesting the following reaction:

$$2LiNH_2 + MgH_2 \leftrightarrow Li_2Mg(NH)_2 + 2H_2 \quad (5)$$

PCI (Pressure-Composition-Isotherm) in desorption for the Li2:Mg1 system at 200 °C resulted in an equilibrium pressure of 32 atm for the main reaction. In the same way, both groups suggested the main reaction to proceed as follows:

$$Li_2Mg(NH)_2 + 2H_2 \leftrightarrow 2LiH + Mg(NH_2)_2 \quad (6)$$

Later in the same year, two other works [61,62] reported the direct synthesis of $Mg(NH_2)_2$ by ball milling of MgH_2 under an atmosphere of NH_3. Afterwards, both groups prepared a mixture of $Mg(NH_2)_2$ with different ratios of LiH (i.e. $Mg(NH_2)_2$:LiH), Nakamori et al. in a Li4:Mg1 ratio and Leng et al. in a Li8:Mg3 ratio. The first group also analysed a mixture of $Mg(NH_2)_2$ plus MgH_2 in Li1:Mg1 and Li2:Mg1 molar ratio for comparison. The results showed that the amide compounds, in the presence of Li-containg phases, presented no NH_3 release. Furthermore, they also reported a total release of 6.5 wt.% H_2 for an experiment conducted up to 600 °C at a heating rate of 10 °C/min under an atmosphere of 1 atm argon. The final products for the decomposition reaction were Mg_3N_2 and Li_3N compounds. In another work [63], authors presented the re-absorption reaction from the final compounds conducted at 250 °C and 350 atm H_2, for the Li4:Mg1 system as:

$$Mg(NH_2)_2 + 4LiH \leftrightarrow 1/3Mg_3N_2 + 4/3Li_3N + 4H_2 \quad (7)$$

On the other hand, Leng et al. have presented for the desorption of the Li8:Mg3 system a completion of the reaction at 400 °C with a total of 7 wt.% H_2 [61]. XRD pattern of the desorbed sample showed other two compounds Li_2NH and Mg_3N_2 as final products. In addition, the re-absorption reaction was conducted at more moderate conditions (200 °C, 30 atm H_2). Initial phases were reformed according to the reversible reaction:

$$3Mg(NH_2)_2 + 8LiH \leftrightarrow Mg_3N_2 + 4Li_2NH + 8H_2 \quad (8)$$

In the sequence of such works, several studies were published following these approaches; i.e. partial substitution of Li by Mg and/or changes in their molar ratios [64].

Moreover, substantial changes in the reaction pathways and intermediate compounds formation were observed as a function of ball milling conditions. Two early works in the Li2:Mg1 system have demonstrated that the intermediate $Mg(NH_2)_2$ and LiH compounds were already formed during ball milling [65,66]. Values reported in the first work for the crystallite sizes of all the identified phases were kept lower than 80 nm after ball milling from 2 to 4 hours [65]. Another study showed that with prolonged milling time (45 h) a scheme of the phase transformations can be written as [66]:

$$2LiNH_2 + MgH_2 \leftrightarrow Mg(NH_2)_2 + 2LiH \leftrightarrow Li_2NH + MgNH + 2H_2 \quad (9)$$

A different picture was observed for the Li1:Mg1 system, with a greater influence of the milling duration, by partial transformation of the system after 12 h of ball milling as follows [67,68]:

$$LiNH_2 + MgH_2 \leftrightarrow 1/2Mg(NH_2)_2 + LiH + 1/2MgH_2 \quad (10)$$

As milling time increased to 48 hours, increase of the vessel pressure was observed and the initial composite resulted into the MgNH + LiH mixture at RT. Hydrogen desorption curves were also shifted to lower temperatures and presented less intense peaks. Moreover, volumetric measurements resulted in total hydrogen release of 6.3 wt.% and 3.2 wt.% for 12 h and 48 h samples, respectively. Results from another study have compared milling time and speed rotations for this same Li1:Mg1 system [69]. The authors reported a different multi-step reaction leading to the $Li_2Mg(NH)_2$ compound for the high energy process in 4 hours, while the low energy ball milling resulted in the complete desorption into single LiMgN. Clearly, discussion still exists regarding both the effects of stoichiometry and milling conditions on the reactions and new phases for the Li-Mg-N system [70].

Just after the first pioneering works in the Li-Mg-N-H system, in 2005 Vajo et al. reported the reversibility of complex hydride ($LiBH_4$) by destabilization with a single metal hydride (MgH_2) [71].

Mechanically milled mixtures of both $LiBH_4/MgH_2$ and LiH/MgB_2 were prepared and studied with addition of 2–3 mol% of $TiCl_3$. An approach on the Li-Mg-B-H system was explored, in which thermodynamic tailoring was achieved with a predicted equilibrium at 255 °C under 1 atm of hydrogen (400 °C for pure $LiBH_4$). It consequently also contributed to a new route for the reformation of $LiBH_4$ under more moderate conditions. The reversible reaction without compromising the hydrogen capacity (11.6 wt.%) of the system was shown to follow:

$$LiBH_4 + 1/2MgH_2 \leftrightarrow LiH + 1/2MgB_2 + 2H_2 \quad (11)$$

Destabilization occurs during dehydrogenation by exothermic formation of MgB_2, which in consequence lowers the endothermic energy barrier for dehydrogenation of $LiBH_4$. Hydrogenation of $TiCl_3$ doped LiH/MgB_2 was demonstrated to occur at ca. 350 °C under 100 atm H_2 after 6 hours, which on subsequent cycles occurred at 300 °C and significantly faster, with more than 9 wt.% uptake in 2 hours. Presence of LiCl was observed in the dehydrogenated products, but not in the

hydrogenated products, due to solubility of LiCl in $LiBH_4$ [49]. Further investigation of the system elucidated the reaction pathway by in-situ XRD, as desorption being a two-step reaction with decomposition of MgH_2 before $LiBH_4$ [72]. In agreement with the first work, hydrogen absorption was observed to occur under moderate isothermal conditions (250–300 °C, 50 atm H_2), whereas the poor kinetics hindered the reaction in dynamic conditions, as evidenced in scanning temperature profiles.

Despite or due to the fact that intense investigation was conducted to understand the reaction pathway, mostly by starting from the hydrogenated state ($LiBH_4$-MgH_2), a variety of conclusions exists in the literature. For example, a backup hydrogen pressure is reported to be crucial in the formation of MgB_2 [73–76]. However, it was also reported that a backup pressure of 3 atm H_2 suppresses the individual decomposition of $LiBH_4$ up to 450 °C [77]. Furthermore, presence of MgB_2 after desorption was pointed as necessary for the formation of $LiBH_4$ and for the reversibility of the reaction [78,79]. Nonetheless, other results under dynamic vacuum have shown a desorption reaction with the formation of Li-Mg alloys instead of MgB_2 and thus a partial reversibility [80,81,82]. Additionally, recent results showed that interfacial volume was always higher in the catalyzed system; a parameter which is expected to govern mass transport and lead to improvements on H_2 sorption rates [83].

In addition, Barkhordarian et al. have demonstrated that composites of MgB_2 with other binary hydrides (NaH, CaH_2) can also enhance hydrogenation to their related boron hydrides ($NaBH_4$, $Ca(BH_4)_2$) [84]. This approach, called Reactive Hydride Composites (RHC), has been extended to other materials systems for hydrogen storage in the solid state. For clarification, the reactive term was given after the ball milling process, which in some cases may be conducted under reactive atmosphere, and composite, after the combination of two or more different hydrides.

3. The Na-Mg-B-H system as case study

Finally, the Na-Mg-B-H system is here comprehensibly described, as it was considered a model system among reactive hydride composites [85]. Pure $NaBH_4$ has been suggested as the exemplary borohydride and even signed as fuel of the future [86], despite known barriers for practical applications, such as its high stability for thermolysis and difficult regeneration of products from hydrolysis. Nevertheless, this RHC was considered a model system for reasons of its high hydrogen capacity and its low costs.

Investigation has been conducted on the sorption reactions starting from $NaBH_4$-MgH_2 system as a function of temperature and pressure, such as correlating structural and thermodynamic aspects by ex-situ and in-situ characterization techniques. Ideally, this hydride composite decomposes before melting, so it was used as an ideal system for studying kinetics of RHC material system [100]. The absorption in the NaH-MgB_2 system has gained more focus regarding the influence of stoichiometry in the mechanism and reactions pathway.

Structural and thermodynamic properties of the up-to-now known solid crystalline phases in the Na-Mg-B-H system (see Table 3) was taken from available databases (ICSD, NIST/ JANAF, ASM), as well as from more recent literature, as will be discussed in more detail in the following sections.

Table 3. Solid crystalline phases in the Na-Mg-B-H system.

System						***Structure***		***Thermodynamics***	
					Chemical Formula	Space Group	Hydrogen, wt.%	ΔH_f^o, kJ/mol f.u.	$T_{transf.}$, °C
Unary	Na				Na	*Im3m*	-	25.6	98
	Mg				Mg	*P63mmc*	-	35.0	649
	B				B	*R3mr*	-	136.5	2027
	H				-	-	-	-	-
Binary	Na	B			NaB_{15}	*Imma*	-	-	-
		H			NaH	*Fm3m*	4.20	56.4	427
		Mg			-	-	-	-	-
	Mg	B			MgB_2	*P6mmm*	-	92.0	830
					MgB_4	*Pnma*	-	105.0	-
					MgB_7	*Imam*	-	-	-
		H			MgH_2	*P42mnm*	7.66	76.1	287
	B	H			-	-	-	-	-
Ternary	Na	Mg	B		-	-	-	-	-
			H		$NaMgH_3$	*Pnma*	6.06	141.0	371
		B	H		NaB_3H_8	*Pmmn*	12.7		
					$NaBH_4$	*Fm3m*	10.66	191.8	497
					$Na_2B_{12}H_{12}$	*P121n1*	6.44	-	-
	Mg	B	H		$Mg(BH_4)_2$	*P6122*	14.94		
					$Mg(B_3H_8)_2$	*P1*	15.31	-	-
					MgB_3H_7	*P1*	11.06		
Quaternary	Na	Mg	B	H	-	-	-	-	-

$T_{transf.}$: temperature of melting/ decomposition.

Pure sodium, at 1 atm, melts at 98 ˚C and remains liquid up to 883 °C with excellent heat transfer properties. Whereas pure magnesium, at 1 atm, melts a much higher temperature of 649 °C [87]. The two together, Na-Mg, do not form alloys of any kind and present poor solid solubility of 7.2 wt.% Mg in liquid Na. Pure boron, at 1 atm, may take either an amorphous form or crystalline in different crystallographic phases (α, β: rhombohedral and γ: tetragonal). According to ASM handbook of binary alloys, there is no assessed B-H or B-Na phase diagrams, but there are six known phases between boron and hydrogen (B_5H_4-I4/acd, B_9H_{11}-P21/c, $B_{10}H_{13}$-P2/n, B_7H_{10}-P222, B_2H_3-Pbca, BH_3-P2/n) and only one reported phase between boron and sodium (NaB_{15}). Phase diagram of B-Mg is known (since 1988) particularly due to the interesting super-conducting properties at low temperatures of the MgB_2 phase. Phase diagrams for binary hydrides (Na-H and Mg-H) are also known (since 1968 and 1987) and have been recently assessed and up-dated [88]. Phase diagrams for ternary systems (Na-B-H and Mg-B-H) have not been confirmed for the range of temperatures and pressures for hydrogen storage [89] with experimental results, except for a recent

phase stability map of the Na1-Mg1-H3 system [90]. In the literature it can be also found calculated in different temperatures and pressures (Figure 1) for the phases in equilibrium for the quaternary Na2-Mg1-B2-H10 system [91].

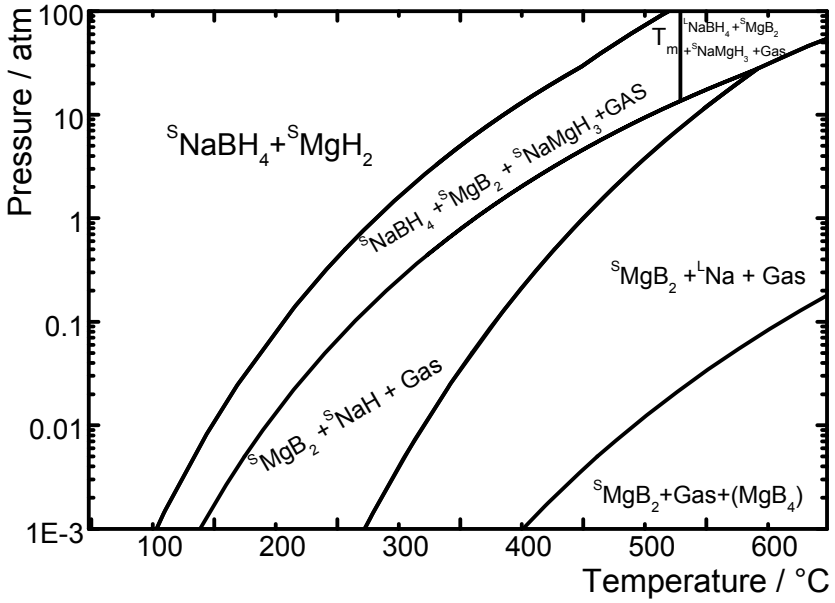

Figure 1. Phase diagram of Na2-Mg1-B2-H10 system.

Overall sorption reaction for the reactive hydride composite of the Na-Mg-B-H system was proposed as follows (8.0 wt.%):

$$2NaBH_4 + MgH_2 \leftrightarrow 2NaH + MgB_2 + 4H_2 \qquad (12)$$

with ΔH_o = 64 kJ/mol$^{-1}H_2$, ΔS_o = 102 J/K.mol H_2 and T_{eq} = 360 °C (in 1 atm H_2). It is considered a solid-state reaction as temperature is below the melting point (Table 3) of all the equilibrium phases. Thus, usually, the main reaction $NaBH_4$-MgH_2/NaH-MgB_2 is assumed as a displacive solid-state transformation, in which phases develop by inter-diffusion and atoms rearrangement, in comparison to a reconstructive kind of transformation with complete breaking and re-buiding of chemical bonds. Complete release of hydrogen (+2.0 wt.%) would lead to the following reaction (l: liquid):

$$2NaH + MgB_2 \leftrightarrow 2Na_{(l)} + 2MgB_2 + H_2 \qquad (13)$$

with ΔH_o = 112 kJ/mol$^{-1}H_2$, ΔS_o = 153 J/K.mol$^{-1}H_2$ and T_{eq} = 427 °C (in 1 atm H_2). This reaction occurs in the presence of a liquid phase (Na), which, as already discussed, presents a solubility of Mg up to 7.2 wt.% and may leave small amounts of amorphous boron. However, if considered the ternary hydride ($NaMgH_3$), as in the assessed thermodynamic values, a different reaction pathway may be expected for the Na2-Mg1-B2-H10 system.

Regarding the pure $NaBH_4$, an early detailed study on the decomposition reaction leading to the pure elements (Na, B, H_2), reported a melting point of 497 °C under a range of pressures from 1 to

10 atm of H_2 [92]. This primary finding is supported by a recent work that additionally reports equilibrium measurements of the pure borohydride, which gives a formation enthalpy of 108 $kJ.mol^{-1}H_2$ and an entropy of 133 $J.K^{-1}mol^{-1}H_2$ [93]. Additionally, ab-initio calculations coupled with experiments recently indicated that partial dehydrogenation of $NaBH_4$ takes place at lower temperatures depending on the applied pressure [94]. More recently, decomposition of pure $NaBH_4$ was reported at lower temperatures and with reversibility by using Ti-based [95] and Ni-based [96] catalysts, respectively. Moreover, adding only small quantities of boron, resulted in lowering the rate of hydrogen release before the melting temperature [97].

Regarding the intermediate phases, closo-dodecaborate compounds have been experimentally observed in the thermal decomposition of pure $NaBH_4$ [98,99], $Mg(BH_4)$, and other borohydrides (e.g. $LiBH_4$) [100,101,102]. Ab-initio calculations show that these [$-B_{12}H_{12}^{2-}$] compounds are likely to be products from decomposition of pure borohydrides. For the mixed systems, both closo-dodecaborate ($CaB_{12}H_{12}$) and ternary hydride ($Ca_3Mg_4H_{14}$) was observed during desorption of $CaBH_4$-MgH_2 as intermediate and side-product phases, respectively [103]. More recently, both $CaB_{12}H_{12}$ and $Li_2B_{12}H_{12}$ were claimed to be the by-products responsible to lower the performance of an eutectic mixture of $0.68LiBH_4$–$0.32Ca(BH_4)_2$ [104]. In fact, formation of $Li_2B_{12}H_{12}$ during hydrogen desorption in the $LiBH_4$-MgH_2 system can be supressed by using NdF_5 as dopant, with a certain backup pressure [105,106]. These are all very recent work and more understanding of intermediate and by-product phases is still under progress.

Similarly, for the $NaBH_4$-MgH_2 system, intermediate phases, such as $Na_2B_{12}H_{12}$, was experimentally observed during desorption under different range of conditions [107]; and the hydride $NaMgH_3$ between 350 and 450 °C—during desorption under vacuum conditions [108], during absorption from 5 to 50 atm hydrogen pressures [109], and during re-absorption under 50 atm hydrogen [110]. Intermediate phases and reaction pathways will be discussed in more detail as a function of experimental conditions used for both hydrogen desorption and absorption in the Na-Mg-B-H system.

3.1. Desorption reactions—of the $NaBH_4/MgH_2$

As early as 2004, a work in the superconductivity field had reported an alternative synthesis route for the production of ultrafine MgB_2 powder through a claimed solid-state reaction between $NaBH_4$ and $MgCl_2$ (5:1 molar ratio) [111]. Experiments conducted in an autoclave at 600 °C with an internal pressure of 200 atm H_2, resulted in the decomposition of the initial compounds, followed by reactions between BH_3 and NaH and then HCl- NaH, according to the overall reaction (g: gaseous):

$$2NaBH_4 + MgCl_2 + H_2 \leftarrow 400\ °C \rightarrow 2NaH + 2HCl_{(g)} + 2BH_{3(g)} \qquad (14)$$

$$\leftarrow 600\ °C \rightarrow MgB_2 + 2NaCl + 2H_2$$

After autoclave, the resulting black powder was washed with a solution of ethanol and water and dried in vacuum at 60 °C for 4 hours. Characterization of the black powder confirmed by XRD pattern to be MgB_2, with a hexagonal structure with a 2.05 B to Mg ratio, measured by XPS, morphology being ultrafine particles of 300 nm, determined by TEM analysis. Similar features of the MgB_2 powder are also observed in commercial products from more routinely used synthesis routes.

Later, ball milling of $NaBH_4$ and $MgCl_2$ in a molar ratio of 2:1 resulted in different products as reported by Varin et al. [112]. The metathesis reaction was expected to proceed as follows:

$$2NaBH_4 + MgCl_2 \leftrightarrow Mg(BH_4)_2 + 2NaCl \quad (15)$$

Instead they show a detail study on the solubility of Mg into $NaBH_4$ supported by a progressive shift of the Bragg peaks in the XRD patterns as a function of ball milling time of the (Na-Mg)BH_4 solid solutions. This hypothesis is sustained by the presence of additional DSC peaks, but which could also be assigned to a disordered $Mg(BH_4)_2$. Moreover, formation of neither NaH nor MgB_2 is mentioned in that study as product compounds in any stage of the reaction. Earlier works, performed by the same group, reported the formation of MgB_2 from decomposition reaction of MgH_2 in the presence of pure $NaBH_4$ [113]. A mixture of MgH_2 and pure $NaBH_4$ was produced by ball milling of Mg under hydrogen pressure with small fractions of $NaBH_4$ (2, 10 and 20 wt.%) [114]. In this case, DSC profiles have shown a strong destabilization effect of $NaBH_4$ and a decrease of the desorption temperature of the MgH_2, as compared with the as received sample. In addition to the MgB_2 formation, which played an important role in the destabilization of the system, they also observed an expansion in the unit cell of the final Mg phase, attributed to the solid solution of Na atoms into the structure. This metathesis reaction is a common method for the synthesis of $Mg(BH_4)_2$, even though it can be synthetized also by other routes. More importantly, magnesium tetrahydroborate remains one of the most promising materials for H_2 storage due to high hydrogen capacity (14.9 wt.%) and good thermodynamics (40 $kJ.mol^{-1}$). Thus, understanding the phase stability of the Na-Mg-B-H system may be of fundamental importance for future applications.

A systematic study is shown in recent book by Varin et al. [22], in which these aspects are discussed based on the rule of mixtures (ROM), commonly known and used for composite materials. Thus, the ROM was extended to RHCs and, in particular, to the MgH_2-$NaBH_4$ system by following the main expected reaction leading to MgB_2-NaH (reaction 12). Hydrogen desorption temperature of the composite, compared to pure $NaBH_4$, can be predicted by the ROM [94]. Authors suggested that decrease in the desorption temperature of $NaBH_4$ coincides with the appearance and increase of pure Mg, suggesting its catalyst effect [115]. This hypothesis was tested with $NaBH_4$-Mg mixtures and, apart from the 92 wt.% Mg case, results followed closely to the ones obtained for MgH_2. While morphology of the mixtures is characterized by the presence of clusters, for the sample containing 92 wt.% Mg, milling was reported to be rather ineffective. Therefore, it was assumed that insufficient contact between the particles results in lower destabilizing effect of the hydrides.

By in-situ synchrotron XRD, Garroni et al. have demonstrated that the above reaction starts at as low as 320 ºC, with the desorption of MgH_2 leaving pure Mg, and then proceeds via chemical decomposition of $NaBH_4$ into NaH and an intermediate species, leaving MgB_2 as one of the final reaction products [116]. They proposed that the reaction mechanism is possibly intermediated by a B-rich phase $Na_2B_{12}H_{12}$ [99]. As previously mentioned, this very stable dodecahydrododecaborate phase, appearing as by-product, is possibly hindering the reaction, because of a very high enthalpy of formation [117]. This first in-situ XRD study suggests that desorption reaction of the $2NaBH_4$+MgH_2 composite passes by an intermediate step under static vacuum, as follows:

$$2NaBH_4 + MgH_2 \leftrightarrow Mg + 2NaBH_4 + H_2$$

$$\leftrightarrow 1/6NaB_{12}H_{12} + 5/3NaH + Mg + 19/6H_2 \quad (16)$$

$$\leftrightarrow 2NaH + MgB_2 + 4H_2$$

It is worth to mention that the suggested NaH phase, however, was not experimentally observed among the final products in this study. A later work by Garroni et al. [107], conducted with NMR technique, has confirmed the presence of an amorphous phase $Na_2B_{12}H_{12}$ in the Na2:Mg1 system for a partially desorbed sample after 2 hours at 450 °C under static pressure of 1 atm Argon. Remarkably, in this later work, the complete desorption into pure Na was confirmed, which appears as a liquid phase, evidenced by a broad X-ray diffraction halo in the high d-spacing range.

Experimental equilibrium measurements were also performed to determine thermodynamics of the decomposition reaction of $2NaBH_4 + MgH_2$. Mao et al. have conducted isotherms at 470, 510 and 560 °C in a TiF_3-doped RHC, resulting in a Van't Hoff diagram with enthalpy of 100.58 kJ/mol H_2 [95]. For the non-equilibrium measurements, a partially desorbed sample at 380 °C resulted only in $NaBH_4$ and Mg. Further heat treatment up to 600 °C under 40 atm H_2 leaded to final products, i.e. NaH and MgB_2. Most likely, NaH may have formed during cooling under hydrogen pressure. Moreover, the hydrogen content released during desorption showed in their results reached about 10 wt.%, which corresponds to the total desorption into pure Na and not to NaH. Subsequently, another work has also been reported with 9 wt.% hydrogen for the desorption reaction of the 2:1 system [118]. In the same study, formation of $NaMgH_3$ was observed during the re-absorption at 450 °C and 50 atm H_2 for 1 hour. The origin of the formation of this ternary hydride was assumed to come from the breaking of the Mg-B bonds from the reaction MgB_2 + Na/NaH during the heating at 450 °C under 50 atm H_2. Since higher temperature (830 °C) is needed to break the Mg-B bond in pure MgB_2, it is plausible that the interaction between Na/NaH and MgB_2 results in a decrease of the decomposition temperature for the single compounds. At this point, the Mg and B elements are able to react with the sodium/sodium hydride counterparts, to produce $NaMgH_3$ and $NaBH_4$, respectively, as evidenced in the XRD patterns. Additionally, it was also shown that the desorption kinetics can be improved by simply changing the stoichiometry of the composite. While the system $NaBH_4$:$2MgH_2$ desorbs in 3 hours, the $2NaBH_4$+MgH_2 desorbs in 20 hours suggesting a principal role of MgH_2 in the destabilization of $NaBH_4$, with a 6.0 wt.% hydrogen capacity. A systematic ex-situ work of $2NaBH_4$:MgH_2 under static vacuum has shown different mechanisms for the main desorption reaction pathway as confirmed by different techniques such as XRD, IR, and SEM [119,120]. Sequence of the formed phases, as a function of temperature, has been schematically represented according to their respective weight percentage (Figure 2).

Traces of $NaMgH_3$ were observed in the temperature range between 350–450 °C, suggesting the occurrence of secondary reactions. Such reactions may compete and hinder the development of main expected phases, by lowering the hydrogen desorption within the system. Formation of additional phases that lead to the release of amorphous boron may be the reason for the observed poor kinetics and reversibility of this RHC system. After that, a detail investigation of pure $NaMgH_3$ was performed by including a reassessment of the thermodynamic and structural characteristics by both experimental analysis and ab-initio calculations [90].

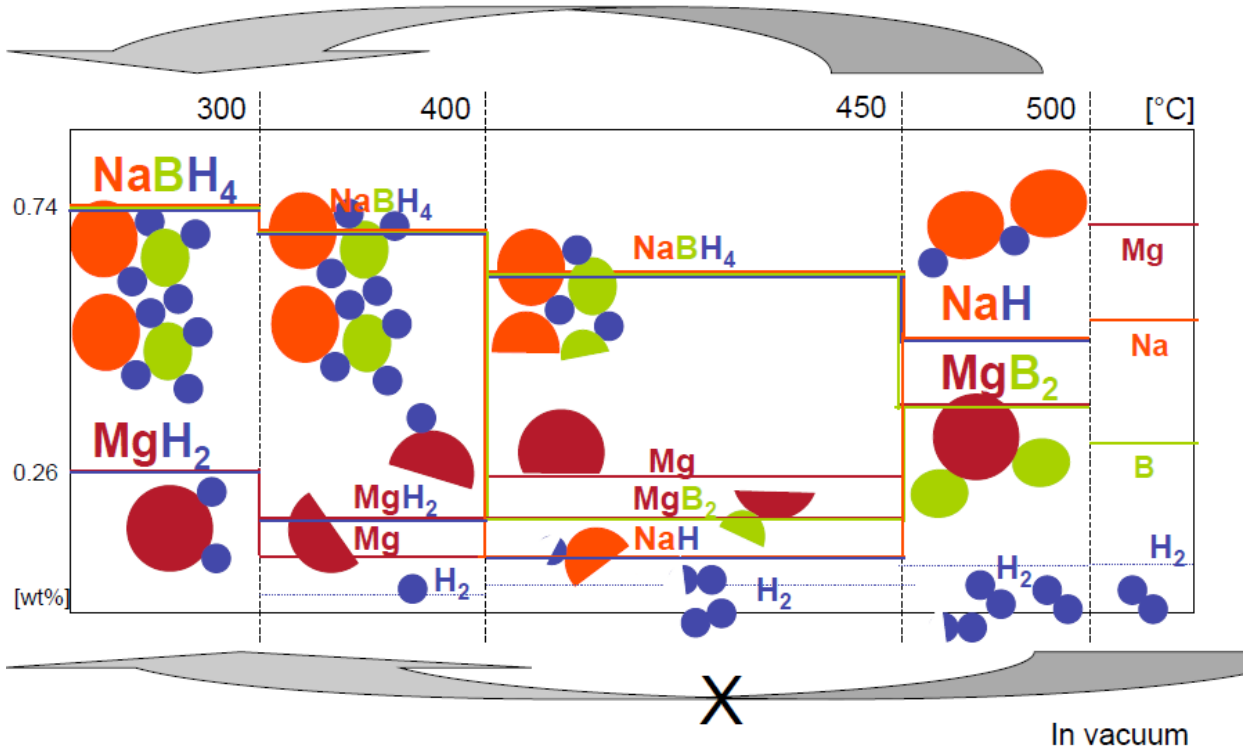

Figure 2. Schematic pathway for desorption reactions of $2NaBH_4/MgH_2$–$2NaH/MgB_2$.

Structural and microstructural evolution of $2NaBH_4 + MgH_2$ desorption were also characterized by SEM and TEM techniques [121]. Initial particles size distribution was identified to be divided into two domains, with ranges of 5–10 μm and 20–30 μm. Particle size range is apparently the same after partial desorption at 350 °C in 0.1 atm H_2, with pure Mg as an intermediate phase. Total hydrogen desorption was carried out in 0.1 atm H_2 pressure from room temperature up to 450 °C at a heating rate of 3 °C/min, and reported to be achieved in two steps with the total hydrogen release of 7.84 wt.%. By these SEM-TEM investigations, desorption reaction of the system was proposed to be kinetically restricted and limited by the growth of MgB_2 at the $Mg/Na_2B_{12}H_{12}$ interface, where the intermediate product phases form a barrier to diffusion. During desorption, MgB_2 particles are observed to grow as plates through intermediate steps, involving Mg and B species around NaH particles. By in-situ neutron diffraction technique, it was shown that the first step of desorption for a ball milled $2NaBH_4$-MgH_2 starts at lower than 250 °C under vacuum conditions, with only pure Mg as main crystalline identified phase [120]. As mentioned before, the presence of pure Mg consequently seams to destabilize the decomposition of pure $NaBH_4$. As reported by Mao et al., Mg is as effective as some additives (TiO_2, Zr, Si, BCC alloy), except for doped-TiF_3 sample which demonstrated better destabilization by decrease of decomposition temperature (ΔH = 100.58 kJ/mol H_2) and enhance reversibility at 600 °C and 40 atm [122].

Nuclear magnetic resonance (NMR) has being highly effective in assessing amorphous phases, sorption temperatures and to understand reaction mechanisms in materials for hydrogen storage, particularly when coupled with DFT calculations. For example, the presence of ($B_{12}H_{12}^{2-}$) compounds were first confirmed by NMR measurements [102]. Onset temperature of dehydrogenation of $NaBH_4$ by formation of MgB_2 was detected at 345 ºC in the composite Na2:Mg1

system [123]. Moreover, ^{1}H and ^{23}Na NMR measurements performed on pure $NaMgH_3$, showed peak narrowing already at 100 °C, with the fraction of spins in the narrow component grows to 100% near 275 °C. After annealing at 400 °C, the intensity of the narrow component was substantially reduced at temperatures below 200 °C; therefore, it appears that the high rates of H motion are due to regions with poorly organized crystal structure. If this disorder could be maintained, this may be an avenue toward improving reaction kinetics of these hydrides [124]. Very recently, another phase studied by ^{11}B NMR was NaB_3H_8 during thermolysis. This sodium borane with high hydrogen capacity was confirmed to decompose into $NaBH_4$ and $Na_2B_{12}H_{12}$ [125]. These late findings introduce a further discussion about the nature and role of boranes on the $NaBH_4$-based or other borohydride systems, extending also to amino-boranes.

Using DFT calculations, the stability and mobility of the most prominent lattice defects in the pure $NaBH_4$ and in the RHC system was reported [126]. At experimental dehydrogenation conditions, the Schottky defects of missing Na^+ and BH_4^- ions form the main vehicle for mass transport in $NaBH_4$. Substituting a BH_4^- by an H^- ion yields the most stable defect, locally converting $NaBH_4$ into NaH and most likely occurring at the surface of $NaBH_4$, with release of BH_3. Adding Mg or MgH_2 to $NaBH_4$ promotes the delivery of the BH_3 molecules, originating from the decomposition in the gas phase and formation of B_2H_6 (diborane) molecules. Alternatively, they may decompose immediately to form hydrogen and B. The presence of Mg, and its subsequent conversion into MgB_2, presents a strong driving force for the formation of BH_4^- vacancies in $NaBH_4$ and the substitution of BH_4^- by H-, which boosts the decomposition scenario sketched above. The formation of H divacancies ($B_2H_6^{2-}$ ions) in the lattice obstructs mass transport of B-related species, as divacancies are immobile. In the presence of Mg/MgB_2, these vacancies are relatively less important.

Environmental contamination by O_2/H_2O has also been reported to play a role during desorption reactions in some extent, though pure Mg has always been verified as an intermediate phase [119]. It has been discovered and patented that short-term exposure to a moist atmosphere has a very beneficial effect on the desorption reaction of the $2NaBH_4$-MgH_2 mixture. The activation consist of $NaBH_4$ forming a slurry which wets the MgH_2 particles and resulting in a favourable reaction interface conserved in the solid state even after drying process [127].

In addition, it is observed that kinetics constraint the composite reactions which under certain conditions results in the incomplete reaction of a hydride composite. The interface reactions in the composite reaction were analysed by in-situ X-ray photoelectron spectroscopy and by simultaneously probing D_2 desorption from $NaBD_4$ and H_2 desorption from MgH_2. The observed destabilisation is in quantitative agreement with the calculated thermodynamic properties, including enthalpy and entropy [128]. The results are discussed with respect to kinetic limitations of the hydrogen desorption mechanism at interfaces. From the change of the total surface area and its composition, it has been recently shown that the migration of metallic Mg is significantly retarded due to the formation of passivation layers at interfaces, particularly for the products MgB_2 and NaH [129]. However, it is well known that the kinetic barrier may be overcome by increasing the reaction fronts and shortening the diffusion path of reactants.

A possible way to promote the hydrogen sorption reactions under moderate temperatures and pressures can be reached with the use of additives. Several additives (fluorides; chlorides; hydroxides) have been tested for Na2:Mg1 and Na1:Mg1 systems during desorption [130]. In the Na2:Mg1 mixture, the borohydride decomposition has been shown to take place mainly in liquid state. Among all the investigated additives, MgF_2 is found to improve the desorption kinetics of both the

composites and to reduce the decomposition temperature and enthalpy of $NaBH_4$ in the 2:1 system. These improvements have been also observed for the pure $NaBH_4$ with Ti-based additives and it was found that TiF_3 presents the best catalytic effect. This has been attributed to the substitution of isostructural anions H^-/F^- by positively tuning the thermodynamics, which is explored fully in novel systems based on fluorine compounds [131]. Reversibility of pure $NaBH_4$ has been also reached with Ni-containing nanoparticles, and by using a core-shell strategy [132]. Nanoconfinement of reactive composites obtained by different routes has been efficient on the destabilization of the Na-Mg-B-H system, by both decreasing the hydrogen release temperature and improving desorption kinetics. Regarding the use of combined nanoconfinement and additives in the composite system, NbF_5 is up-to-now found to be the most effective in reducing the decomposition temperature of $NaBH_4$ within the MgH_2-composite [133,134]. A remark worth to mention is that a latest study on phase transformations by hydriding nanocrystals has shown that the adsorption/desorption rate is determined by three factors: pressure, temperature and nanocrystal size; with no significant effect of additional factors such as defects and strain as previously suggested [135].

3.2. Absorption reactions—of the NaH/MgB_2

Evidently, formation of borohydride is the main barrier in order to hydrogenate these composite systems. Regarding synthesis of pure borohydrides or tetrahydoborates, a first description appeared in the literature in 1940 by Schlesinger et al. [136]. They synthesized $AlBH_4$ by a reaction with trimethylaluminum ($Al_2(CH_3)_6$) and diborane (B_2H_6), which was later extended to $LiBH_4$ [137], $NaBH_4$ and KBH_4 [138], and others compounds [139]. Nowadays, the chemical industry synthesizes these compounds by wet chemical reaction involving ethereal solvents or isopropyl amines, requiring extra treatment of liquid by-products. For this reason, a solid-state synthesis would produce a desirable solvent free process for industry. By itself synthesis of (-BH_4) compounds would be thermodynamically favoured as they present a high formation enthalpy (> 50 kJ/mol H_2) [140,141], however, a significant activation barrier has to be overcome due to chemical inertness of pure boron. Pure boron presents a structure with atoms strongly bonded and the presence of a passivating oxide layer on its surface.

By using the RHC approach, formation of borohydrides have been successfully obtained by hydrogenation of MgB_2 together with respective hydrides (LiH [142], MgH_2 [143,144], CaH [145]). In the first study, two different conditions were explored, resulting in $LiBH_4$, $NaBH_4$, and $Ca(BH_4)_2$ among all the trials (MgH_2, ZrH_2, YH_3, LaH_3, NdH_3 or PrH_3 added) using both MgB_2 and Boron [84]. Barkhordarian et al. have shown results far from thermodynamic equilibrium conditions (Reaction 12). Starting from a ball milled sample of 2NaH + MgB_2, almost complete absorption into 2$NaBH_4$ + MgH_2 was reached only under very extreme conditions (300 ºC/ 200 atm/ 48 h and 400 ºC/ 350 atm/ 24 h). In addition, the same work has also shown another phase assigned to minor peaks in the XRD pattern of the reabsorbed samples, suggested as an impurity resulting from NaH oxidation. However, further studies conducted in more detail on the absorption reaction of the Na-Mg-B-H system have observed this unknown phase by in-situ XRD, TEM, and NMR [146]. Mostly, this phase appeared almost simultaneously with the formation of amorphous content and complex interface. In addition, from a mixture of 2NaH-MgB_2, direct mechanochemical synthesis of $NaBH_4$, with minor traces of MgH_2, was observed after milling for 20 hours at slow speed of 300 rpm under 120 atm H_2 [147]. Assessment of the free energy, using CALPHAD, suggested that a hydrogen pressure from

1 to 120 atm at RT promotes nucleation of product phases ($NaBH_4$, MgH_2) by an increase of the driving force of about 10 kJ/mol H_2.

Pistidda et al. have studied extensively the NaH-MgB_2 composite with different stoichiometry (x: 0.5–2.0) [109], at several temperatures and hydrogen pressures (5–50 atm). Melting of a NaH−$NaBH_4$ salt mixture has been observed at 383 ºC regardless of the pressure. They have reported the unknown phase being formed at higher pressures, but not at lower pressures. Later, this unknown phase could be almost purely synthesised and then by XRD coupled with DFT calculation was assigned to a new B-rich cubic phase [129].

A microstructural analysis of the 2NaH-MgB_2 system milled for 1 hour under argon atmosphere was conducted by TEM combined with PCT measurements [146,148]. Samples were heated up to 400 ºC in 50 atm H_2, then held in isothermal conditions for a minimum of 3 hours. At these conditions, onset temperature for absorption reaction was observed at 250 ºC, however, total uptake reached only 3.8 wt.% (total of 8.0 wt.%) in two steps (0.6 wt.% and 3.2 wt.%). The first uptake coincides with the formation of an unknown phase from as low as 190 ºC up to about 320 ºC, temperature after which it disappears. This precedes formation of $NaMgH_3$ from free Mg and NaH at about 330 ºC. Finally, the appearance of crystalline $NaBH_4$ is observed at about 380 ºC together with pure Mg. Based on this early work with the unexpected formation of $NaMgH_3$, Nwakwuo et al. have reported a system with better kinetics compared to 2NaH + MgB_2 [121]. The system 3NaH-MgB_2 with a theoretical hydrogen intake of 6.4 wt.% and equilibrium at 300 ºC under 1 atm H_2 (= 44.3 kJ/mol H_2) was proposed to proceed during absorption as follows:

$$3NaH + MgB_2 + 4H_2 \leftrightarrow 2NaBH_4 + NaMgH_3 \quad (17)$$

Formation of the ternary hydride seems to enhance the absorption reaction to attain full hydrogen capacity as a consequence of the rapid hydrogen motion in $NaMgH_3$ compared to that in MgH_2. The perovskite structure enables such faster hydrogen motion at a broad temperature range, and thereby acts as fast hydrogen diffusion pathways to enhance hydriding/dehydriding reactions. Aadditionally, it has also shown to possess fast hydrolysis reaction kinetics without any passivation [149]. This and other features of $NaMgH_3$ enhance also the reversibility performance of promising composite systems such as $NaAlH_4$-MgH_2 [150], $NaNH_2$-MgH_2 [151], and very recently $LiNH_2$-$NaMgH_3$ was suggested as a novel material system for hydrogen storage [152].

4. Prospective on materials for solid hydrogen storage

A summary of the most relevant findings obtained is given for the solid materials being considered as hydrogen storage medium. Particularly, structural and thermodynamic properties have been discussed for the Na-Mg-B-H system as a case study for hydrogen storage material in the solid state. Other composite systems also present some interesting characteristics for certain applications. In such novel area as materials for hydrogen storage, vigorous research and new breakthrough will be necessary for further development of a suitable system for practical and sustainable applications. Consequently, introduction and adaptation of approaches and experimental techniques have been observed in the hydrogen storage field. Available methods have been developed to a point where almost any property can be measured with good accuracy. Even if an ever more comprehensive knowledge of the properties and reactions of these hydrogen storage materials have answered some

fundamental questions, they are also nurturing and imposing new questions and research directions. For example, hydrogen diffusion has been studied during sorption reactions, but may also in the future give insights about embrittlement behaviour and safety evaluation during application. Thus, it is fundamental to reach understanding of experimental data and computation results from a conceptual to a more practical perspective. In material sciences and engineering, achievements will probably be bigger and faster if researchers get aware of the complexity, interaction and interconnections related to a sustainable hydrogen-based society.

Acknowledgments

D.P. thanks the University of Nottingham and CNPq/CAPES for financial support. This study was partially supported by the EU-FP6 project COSY (MRTN-CT-2006-035366).

Conflict of Interest

All authors declare no conflicts of interest in this paper.

References

1. Crabtree GW, Dresselhaus MS, Buchanan MV (2004) The Hydrogen Economy. *Phys Today* 57: 39–44.
2. Zuttel A, Borgschulte A, Schlapbach L (2008) Hydrogen as a Future Energy Carrier. Winheim: Wiley-VCH Verlag GmbH & Co.
3. Riis T, Hagen EF, Vie PJS, et al. (2006) Hydrogen Production R&D. Paris: IEA.
4. Turner JA (2004) Sustainable Hydrogen Production. *Science* 305: 972–974.
5. Merle G, Wessling M, Nijmeijer K (2011) Anion exchange membranes for alkaline fuel cells: A review. *J Membrane Sci* 377: 1–35.
6. Giddey S, Badwal SPS, Kulkarni A, et al. (2012) A comprehensive review of direct carbon fuel cell technology. *Prog Energy Combust* 38: 360–399.
7. Antolini E, Perez J (2011) The use of rare earth-based materials in low-temperature fuel cells. Int *J Hydrogen Energy* 36: 15752–15765.
8. Stambouli AB, Traversa E (2002) Solid oxide fuel cells (SOFCs): a review of an environmentally clean and efficient source of energy. *Renew Sust Energy Rev* 6: 433–455.
9. Riis T, Sandrock G, Ulleberg O, et al. (2006) Hydrogen Storage R&D. Paris: IEA.
10. Elam CC, Padró CEG, Sandrock G, et al. (2003) Realizing the hydrogen future: the International Energy Agency's efforts to advance hydrogen energy technologies. *Int J Hydrogen Energy* 28: 601–607.
11. MHCoE For a description of the Metal Hydride Center of Excellence. Available from: http://www.sandia.gov/MHCoE.
12. CHCoE For a description of the Chemical Hydride Center of Excellence. Available from: http://www.hydrogen.energy.gov/annual_progress10_storage.html.
13. HSCoE For a description of the Hydrogen Sorption Center of Excellence. Available from: http://www.nrel.gov/basic_sciences/carbon_based_hydrogen_center.cfm#hsce.
14. Klebanoff L (2013) Hydrogen Storage Technology: Materials and Applications. United States of

America: CRC press.
15. US-DOE (2010) Hydrogen and Fuel Cells: Current Technology of Hydrogen Storage. Available from: http://www1.eere.energy.gov/hydrogenandfuelcells/storage/current_technology.html.
16. Felderhoff M, Weidenthaler C, von Helmolt R, et al. (2007) Hydrogen storage: the remaining scientific and technological challenges. *Phys Chem Chem Phys* 9: 2643–2653.
17. Graetz J (2009) New approaches to hydrogen storage. *Chem Soc Rev* 38: 73–82.
18. van den Berg AWC, Arean CO (2008) Materials for hydrogen storage: current research trends and perspectives. *Chem Commun* 14: 668–681.
19. Klebanoff LE, Keller JO (2013) 5 Years of hydrogen storage research in the U.S. DOE Metal Hydride Center of Excellence (MHCoE). *Int J Hydrogen Energ* 38: 4533–4576.
20. Lu Z-H, Xu Q (2012) Recent Progress in Boron and Nitrogen based Chemical Hydrogen Storage. *Functional Materials Letters* 05.
21. Michel KJ, Ozoliņš V (2013) Recent advances in the theory of hydrogen storage in complex metal hydrides. *MRS Bulletin* 38: 462–472.
22. Varin RA, Czujiko T, Wronski ZS (2009) Nanomaterials for solid state hydrogen storage. Cleveland: Springer.
23. Grochala W, Edwards PP (2004) Thermal Decomposition of the Non-Interstitial Hydrides for the Storage and Production of Hydrogen. *Chem Rev* 104: 1283–1316.
24. Eremets MI, Trojan IA, Medvedev SA, et al. (2008) Superconductivity in Hydrogen Dominant Materials: Silane. *Science* 319: 1506–1509.
25. Scheler T, Degtyareva O, Marqués M, et al. (2011) Synthesis and properties of platinum hydride. *Phys Rev B* 83: 214106.
26. Gao G, Wang H, Zhu L, et al. (2011) Pressure-Induced Formation of Noble Metal Hydrides. *J Phys Chem C* 116: 1995–2000.
27. Driessen A, Sanger P, Hemmes H, et al. (1990) Metal hydride formation at pressures up to 1 Mbar. *J Physics: Condensed Matter* 2: 9797.
28. Sandrock G (1999) A panoramic overview of hydrogen storage alloys from a gas reaction point of view. *J Alloys Compounds* 293–295: 877–888.
29. Bogdanovi B, Schwickardi M (1997) Ti-doped alkali metal aluminium hydrides as potential novel reversible hydrogen storage materials. *J Alloy Compd* 253–254: 1–9.
30. Bogdanović B, Brand RA, Marjanović A, et al. (2000) Metal-doped sodium aluminium hydrides as potential new hydrogen storage materials. *J Alloy Compd* 302: 36–58.
31. Eberle U, Arnold G, von Helmolt R (2006) Hydrogen storage in metal–hydrogen systems and their derivatives. *J Power Sources* 154: 456–460.
32. Sandrock G, Gross K, Thomas G (2002) Effect of Ti-catalyst content on the reversible hydrogen storage properties of the sodium alanates. *J Alloy Compd* 339: 299–308.
33. Zaluska A, Zaluski L, Ström-Olsen JO (2000) Sodium alanates for reversible hydrogen storage. *J Allos Compd* 298: 125–134.
34. Gross KJ, Sandrock G, Thomas GJ (2002) Dynamic in situ X-ray diffraction of catalyzed alanates. *J Alloy Compd* 330–332: 691–695.
35. Bellosta von Colbe JM, Felderhoff M, Bogdanovic B, et al. (2005) One-step direct synthesis of a Ti-doped sodium alanate hydrogen storage material. *Chem Commun* 4732–4734.
36. Li L, Xu C, Chen C, et al. (2013) Sodium alanate system for efficient hydrogen storage. *Int J*

Hydrogen Energy 38: 8798–8812.
37. NIST. Availabe from: http://webbook.nist.gov ed.
38. Zaluska A, Zaluski L, Srom-Olsen JO, et al. (1999) Method for inducing hydrogen desorption from a metal hydride. In: 5882623, Patent. United States of America.
39. Zaluska A, Zaluski L, Strˆm-Olsen JO (1999) Nanocrystalline magnesium for hydrogen storage. *J Alloy Compd* 288: 217–225.
40. Varin RA, Czujko T, Wronski ZS, et al. (2009) Nanomaterials for hydrogen storage produced by ball milling. *Can Metall Quart* 48: 11–26.
41. Fichtner M (2009) Properties of nanoscale metal hydrides. *Nanotechnology* 20: 204009.
42. Bérubé V, Radtke G, Dresselhaus M, et al. (2007) Size effects on the hydrogen storage properties of nanostructured metal hydrides: A review. *Int J Energy Res* 31: 637–663.
43. Chen PX, Z.; Luo, J.; Lin, J.; Tan, K. L. (2002) Interaction of hydrogen with metal nitrides and imides. *Nature* 420: 302–304.
44. Hu YH, Ruckenstein E (2003) Ultrafast Reaction between LiH and NH3 during H2 Storage in Li3N. *J Phys Chem A* 107: 9737–9739.
45. Ichikawa T, Hanada N, Isobe S, et al. (2004) Mechanism of Novel Reaction from LiNH2 and LiH to Li2NH and H2 as a Promising Hydrogen Storage System. *J Phys Chem B* 108: 7887–7892.
46. Lohstroh W, Fichtner M (2007) Reaction steps in the Li–Mg–N–H hydrogen storage system. *J Alloy Compd* 446–447: 332–335.
47. Hu YH, Ruckenstein E (2004) Highly Effective Li2O/Li3N with Ultrafast Kinetics for H2 Storage. *Ind Eng Chem Res* 43: 2464–2467.
48. Zuttel A, Wenger P, Rentsch S, et al. (2003) LiBH4 a new hydrogen storage material. *J Power Sources* 118: 1–7.
49. Mosegaard L, Moller B, Jorgensen J-E, et al. (2008) Reactivity of LiBH4: In Situ Synchrotron Radiation Powder X-ray Diffraction Study. *J Phys Chem C* 112: 1299–1303.
50. Yu XB, Grant DM, Walker GS (2009) Dehydrogenation of LiBH4 Destabilized with Various Oxides. *J Phys Chem C* 113: 17945–17949.
51. Maekawa H, Matsuo M, Takamura H, et al. (2009) Halide-Stabilized LiBH4, a Room-Temperature Lithium Fast-Ion Conductor. *J Am Chem Soc* 131: 894–895.
52. Luo C, Wang H, Sun T, et al. (2012) Enhanced dehydrogenation properties of LiBH4 compositing with hydrogenated magnesium-rare earth compounds. *Int J Hydrogen Energy* 37: 13446–13451.
53. Pendolino F (2011) "Boron Effect" on the Thermal Decomposition of Light Metal Borohydrides MBH4 (M = Li, Na, Ca). *J Phys Chem C* 116: 1390–1394.
54. Pendolino F (2013) Thermal study on decomposition of LiBH4 at non-isothermal and non-equilibrium conditions. *J Thermal Analysis Calorimetry* 112: 1207–1211.
55. Gross AF, Vajo JJ, Van Atta SL, et al. (2008) Enhanced Hydrogen Storage Kinetics of LiBH4 in Nanoporous Carbon Scaffolds. *J Phys Chem C* 112: 5651–5657.
56. Xu J, Yu X, Ni J, et al. (2009) Enhanced catalytic dehydrogenation of LiBH4 by carbon-supported Pd nanoparticles. *Dalton Transactions*: 8386–8391.
57. Xu J, Yu X, Zou Z, et al. (2008) Enhanced dehydrogenation of LiBH4 catalyzed by carbon-supported Pt nanoparticles. *Chem Commun* 5740–5742.
58. Xu J, Qi Z, Cao J, et al. (2013) Reversible hydrogen desorption from LiBH4 catalyzed by graphene supported Pt nanoparticles. *Dalton Transactions* 42: 12926–12933

59. Luo W (2004) (LiNH2–MgH2): a viable hydrogen storage system. *J Alloy Compd* 381: 284–287.
60. Xiong Z, Wu G, Hu J, et al. (2004) Ternary Imides for Hydrogen Storage. *Adv Mater* 16: 1522–1525.
61. Leng HY, Ichikawa T, Hino S, et al. (2004) New Metal−N−H System Composed of Mg(NH2)2 and LiH for Hydrogen Storage. *J Phy Chem B* 108: 8763–8765.
62. Nakamori Y, Kitahara G, Orimo S (2004) Synthesis and dehydriding studies of Mg–N–H systems. *J Power Sources* 138: 309–312.
63. Nakamori Y, Kitahara G, Miwa K, et al. (2005) Reversible hydrogen-storage functions for mixtures of Li3N and Mg3N2. *Appl Phys A* 80: 1–3.
64. Dolci F, Weidner E, Hoelzel M, et al. (2010) In-situ neutron diffraction study of magnesium amide/lithium hydride stoichiometric mixtures with lithium hydride excess. *Int J Hydrogen Energy* 35: 5448–5453.
65. Barison S, Agresti F, Lo Russo S, et al. (2008) A study of the LiNH2–MgH2 system for solid state hydrogen storage. *J Alloy Compd* 459: 343–347.
66. Shahi RR, Yadav TP, Shaz MA, et al. (2008) Effects of mechanical milling on desorption kinetics and phase transformation of LiNH2/MgH2 mixture. *Int J Hydrogen Energy* 33: 6188–6194.
67. Liang C, Liu Y, Luo K, et al. (2010) Reaction Pathways Determined by Mechanical Milling Process for Dehydrogenation/Hydrogenation of the LiNH2/MgH2 System. *Chemistry A European Journal* 16: 693–702.
68. Liu Y, Li B, Tu F, et al. (2011) Correlation between composition and hydrogen storage behaviors of the Li2NH-MgNH combination system. *Dalton Transactions* 40: 8179–8186.
69. Lu J, Choi YJ, Fang ZZ, et al. (2010) Effect of milling intensity on the formation of LiMgN from the dehydrogenation of LiNH2–MgH2 (1:1) mixture. *J Power Sources* 195: 1992–1997.
70. Pottmaier D, Dolci F, Orlova M, et al. (2011) Hydrogen release and structural transformations in LiNH2–MgH2 systems. *J Alloy Compd* 509, Supplement 2: S719–S723.
71. Vajo JJ, Skeith SL, Mertens F (2005) Reversible Storage of Hydrogen in Destabilized LiBH4. *J Phys Chem B* 109: 3719–3722.
72. Bosenberg U, Doppiu S, Mosegaard L, et al. (2007) Hydrogen sorption properties of MgH2-LiBH4 composites. *Acta Materialia* 55: 3951–3958.
73. Bosenberg U, Ravnsbk DB, Hagemann H, et al. (2010) Pressure and Temperature Influence on the Desorption Pathway of the LiBH4-MgH2 Composite System. *J Phys Chem C* 114: 15212–15217.
74. Nakagawa T, Ichikawa T, Hanada N, et al. (2007) Thermal analysis on the Li-Mg-B-H systems. *J Alloy Compd* 446–447: 306–309.
75. Shim J-H, Lim J-H, Rather S-u, et al. (2009) Effect of Hydrogen Back Pressure on Dehydrogenation Behavior of LiBH4-Based Reactive Hydride Composites. *J Phys Chem Lett* 1: 59–63.
76. Yang J, Sudik A, Wolverton C (2007) Destabilizing LiBH 4 with a Metal (M) Mg , Al , Ti , V , Cr , or Sc) or Metal Hydride (MH 2). *J Phys Chem C* 111: 19134–19140.
77. Pinkerton FE, Meyer MS, Meisner GP, et al. (2007) Phase Boundaries and Reversibility of LiBH 4 / MgH 2 Hydrogen Storage Material. *J Phys Chem Lett C* 111: 12881–12885.
78. Price TEC, Grant DM, Legrand V, et al. (2010) Enhanced kinetics for the LiBH4:MgH2 multi-component hydrogen storage system—The effects of stoichiometry and decomposition environment on cycling behaviour. *Int J Hydrogen Energy* 35: 4154–4161.

79. Wan X, Markmaitree T, Osborn W, et al. (2008) Nanoengineering-Enabled Solid-State Hydrogen Uptake and Release in the LiBH4 Plus MgH2 System. *J Phys Chem C* 112: 18232–18243.
80. Price TEC, Grant DM, Telepeni I, et al. (2009) The decomposition pathways for LiBD4-MgD2 multicomponent systems investigated by in situ neutron diffraction. *J Alloy Compd* 472: 559–564.
81. Walker GS, Grant DM, Price TC, et al. (2009) High capacity multicomponent hydrogen storage materials: Investigation of the effect of stoichiometry and decomposition conditions on the cycling behaviour of LiBH4‚ÄìMgH2. *J Power Sources* 194: 1128–1134.
82. Yu XB, Grant DM, Walker GS (2006) A new dehydrogenation mechanism for reversible multicomponent borohydride systems--The role of Li-Mg alloys. *Chem commun (Cambridge, England)* 1: 3906–3908.
83. Dobbins T, NaraseGowda S, Butler LG (2012) Study of Morphological Changes in MgH2 Destabilized LiBH4 Systems Using Computed X-ray Microtomography. *Materials* 5: 1740–1751.
84. Barkhordarian G, Klassen T, Dornheim M, et al. (2007) Unexpected kinetic effect of MgB2 in reactive hydride composites containing complex borohydrides. *J Alloy Compd* 440: L18–L21.
85. COSY-network Complex Solid State Reaction for Energy Efficient Hydrogen Storage. Available from: www.cosy-net.eu.
86. Santos DMF, Sequeira CAC (2011) Sodium borohydride as a fuel for the future. *Renew Sust Energy Rev* 15: 3980–4001.
87. Dinsdale AT (1991) SGTE Data for Pure Elements. *CALPHAD* 15: 317–425.
88. Manchester FD (2000) Phase Diagrams of Binary Hydrogen Alloys. United State of America: ASM International.
89. George L, Saxena SK (2010) Structural stability of metal hydrides, alanates and borohydrides of alkali and alkali- earth elements: A review. *Int J Hydrogen Energy* 35: 5454–5470.
90. Pottmaier D, Pinatel ER, Vitillo JG, et al. (2011) Structure and Thermodynamic Properties of the NaMgH3 Perovskite: A Comprehensive Study. *Chem Mater* 23: 2317–2326.
91. Barrico M, Paulmbo M, Pinatel E, et al. (2010) Thermodynamic Database for Hydrogen Storage Materials. *Adv Sci Tech* 72: 213–218.
92. Stasinevich G, Egorenko A (1969) *J Inorg Chem* 13: 341–343.
93. Martelli P, Caputo R, Remhof A, et al. (2010) Stability and Decomposition of NaBH 4. *The J Phys Chem C* 114: 7173–7177.
94. Urgnani J, Torres F, Palumbo M, et al. (2008) Hydrogen release from solid state NaBH4. *Int J Hydrogen Energy* 33: 3111–3115.
95. Mao JF, Yu XB, Guo ZP, et al. (2009) Enhanced hydrogen storage performances of NaBH4-MgH2 system. *J Alloy Compd* 479: 619–623.
96. Humphries TD, Kalantzopoulos GN, Llamas-Jansa I, et al. (2013) Reversible Hydrogenation Studies of NaBH4 Milled with Ni-Containing Additives. *J Phys Chem C* 117: 6060–6065.
97. Pendolino F, Mauron P, Borgschulte A, et al. (2009) Effect of Boron on the Activation Energy of the Decomposition of LiBH4. *J Phys Chem C* 113: 17231–17234.
98. Caputo R, Garroni S, Olid D, et al. (2010) Can Na2[B12H12] be a decomposition product of NaBH4? *Phys Chem Chem Phys* 12: 15093-15100.99. Her J-H, Zhou W, Stavila V, et al. (2009) Role of Cation Size on the Structural Behavior of the Alkali-Metal Dodecahydro-closo-Dodecaborates. *J Phys Chem Lett C* 113: 11187–11189.

100. Friedrichs O, Remhof A, Hwang K-J, et al. (2010) Role of Li2B12H12 for the formation and decomposition of LiBH4. *Chem Mater* 22: 3265–3268.
101. Her JH, Yousufuddin M, Zhou W, et al. (2008) Crystal structure of Li2B12H12: a possible intermediate species in the decomposition of LiBH4. *Inorg Chem* 47: 9757–9759.
102. Hwang SJ, Bowman RC, Reiter JW, et al. (2008) NMR Confirmation for Formation of [B12H12]2- Complexes during Hydrogen Desorption from Metal Borohydrides. *J Phys Chem C* 112: 3164–3169.
103. Minella CB, Pistidda C, Garroni S, et al. (2013) $Ca(BH_4)_2$ + MgH_2: Desorption Reaction and Role of Mg on Its Reversibility. *J Phys Chem C* 117: 3846–3852.
104. Yan Y, Remhof A, Rentsch D, et al. (2013) Is Y2(B12H12)3 the main intermediate in the decomposition process of Y(BH4)3? *Chem Commun* 49: 5234–5236.
105. Mao J, Guo Z, Yu X, et al. (2013) Combined effects of hydrogen back-pressure and NbF5 addition on the dehydrogenation and rehydrogenation kinetics of the $LiBH_4$–MgH_2 composite system. *Int J Hydrogen Energy* 38: 3650–3660.
106. Yan Y, Li H-W, Maekawa H, et al. (2011) Formation of Intermediate Compound Li2B12H12 during the Dehydrogenation Process of the $LiBH_4$–MgH_2 System. *J Phys Chem C* 115: 19419–19423.
107. Garroni S, Milanese C, Pottmaier D, et al. (2011) Experimental Evidence of Na2[B12H12] and Na Formation in the Desorption Pathway of the 2NaBH4 + MgH2 System. *J Phys Chem C* 115: 16664–16671.
108. Pottmaier D, Pistidda C, Groppo E, et al. (2011) Dehydrogenation reactions of 2$NaBH_4$ + MgH_2 system. *Int J Hydrogen Energy* 36: 7891–7896.
109. Pistidda C, Garroni S, Minella CB, et al. (2010) Pressure Effect on the 2NaH + MgB_2 Hydrogen Absorption Reaction. *J Phys Chem C* 114: 21816–21823.
110. Garroni S, Milanese C, Girella A, et al. (2010) Sorption properties of $NaBH_4/MH_2$ (M = Mg, Ti) powder systems. *Int J Hydrogen Energy* 35: 5434–5441.
111. Shi L, Gi Y, Qian T, et al. (2004) Synthesis of ultrafine superconducting MgB2 by a convenient solid-state reaction route. *Physica C* 405: 271–274.
112. Varin RA, Chiu C, Wronski ZS (2008) Mechano-chemical activation synthesis (MCAS) of disordered Mg(BH4)2 using NaBH 4. *J Alloy Compd* 462: 201–208.
113. Varin Ra, Czujko T, Chiu C, et al. (2009) Synthesis of nanocomposite hydrides for solid-state hydrogen storage by controlled mechanical milling techniques. *J Alloy Compd* 483: 252–255.
114. Czujko T, Varin R, Wronski Z, et al. (2007) Synthesis and hydrogen desorption properties of nanocomposite magnesium hydride with sodium borohydride (MgH2+NaBH4). *J Alloy Compd* 427: 291–299.
115. Czujiko T, Varin R, Zaranski Z, et al. (2010) The dehydrogenation process of destabilized NaBH4-MgH2 solid state hydride composites. *Arch Metall Mater* 55: 539–552.
116. Garroni S, Pistidda C, Brunelli M, et al. (2009) Hydrogen desorption mechanism of 2NaBH4+MgH2 composite prepared by high-energy ball milling. *Scripta Materialia* 60: 1129–1132.
117. Caputo R, Garroni S, Olid D, et al. (2010) Can Na2[B12H12] be a decomposition product of NaBH4? *Phys Chem Chem Phys* 12: 15093–15100.
118. Garroni S, Milanese C, Girella A, et al. (2010) Sorption properties of NaBH4/MH2 (M=Mg, Ti) powder systems. *Int J Hydrogen Energy* 35: 5434–5441.

119.Pottmaier D, Garroni S, Barò MD, et al. (2010) Hydrogen Desorption Reactions of the Na-Mg-B-H System. *Adv Sci Tech*72: 164–169.
120.Pottmaier D, Garroni S, Brunelli M, et al. (2010) NaBX4-MgX2 Composites (X= D,H) Investigated by In situ Neutron Diffraction. *Mater Res Soc Symp Proc* 1262: W03–04.
121.Nwakwuo CC, Pistidda C, Dornheim M, et al. (2012) Microstructural study of hydrogen desorption in 2NaBH4 + MgH2 reactive hydride composite. *Int J Hydrogen Energy* 37: 2382–2387.
122.Mao J, Guo Z, Yu X, et al. (2011) Improved Hydrogen Storage Properties of NaBH4 Destabilized by CaH2 and Ca(BH4)2. *J Phys Chem C* 115: 9283–9290.
123.Franco F, Baricco M, Chierotti MR, et al. (2013) Coupling Solid-State NMR with GIPAW ab Initio Calculations in Metal Hydrides and Borohydrides. *J Phys Chem C* 117: 9991–9998.
124.Shane DT, Corey RL, Bowman Jr RC, et al. (2009) NMR studies of the hydrogen storage compound NaMgH3. *J Phys Chem C* 113: 18414–18419.
125.Huang Z, Eagles M, Porter S, et al. (2013) Thermolysis and solid state NMR studies of NaB3H8, NH3B3H7, and NH4B3H8. *Dalton Transactions* 42: 701–708.
126.Çakır D, de Wijs GA, Brocks G (2011) Native Defects and the Dehydrogenation of NaBH4. *J Phys Chem C* 115: 24429–24434.
127.Pistidda C, Barkhordarian G, Rzeszutek A, et al. (2011) Activation of the reactive hydride composite 2NaBH4+MgH2. *Scripta Materialia* 64: 1035–1038.
128.Kato S, Borgschulte A, Bielmann M, et al. (2012) Interface reactions and stability of a hydride composite (NaBH4 + MgH2). *Phys Chem Chem Phys* 14: 8360–8368.
129.Pistidda C, Napolitano E, Pottmaier D, et al. (2013) Structural study of a new B-rich phase obtained by partial hydrogenation of 2NaH + MgB2. *Int J Hydrogen Energy* 38: 10479–10484.
130.Milanese C, Garroni S, Girella A, et al. (2011) Thermodynamic and Kinetic Investigations on Pure and Doped NaBH4−MgH2 System. *J Phys Chem C* 115: 3151–3162.
131.Saldan I, Gosalawit-Utke R, Pistidda C, et al. (2012) Influence of Stoichiometry on the Hydrogen Sorption Behavior in the LiF–MgB2 System. *J Phys Chem C* 116: 7010–7015.
132.Christian M, Aguey-Zinsou K-F (2013) Synthesis of core-shell NaBH4@M (M = Co, Cu, Fe, Ni, Sn) nanoparticles leading to various morphologies and hydrogen storage properties. *Chem Commun* 49: 6794–6796.
133.Mulas G, Campesi R, Garroni S, et al. (2012) Hydrogen storage in 2NaBH4+MgH2 mixtures: Destabilization by additives and nanoconfinement. *J Alloy Compd* 536, Supplement 1: S236–S240.
134.Peru F, Garroni S, Campesi R, et al. (2013) Ammonia-free infiltration of NaBH4 into highly-ordered mesoporous silica and carbon matrices for hydrogen storage. *J Alloy Compd* 580, Supplement 1: S309–S312.
135.Bardhan R, Hedges LO, Pint CL, et al. (2013) Uncovering the intrinsic size dependence of hydriding phase transformations in nanocrystals. *Nat Mater* advance online publication.
136.Schlesinger HI, Sanderson RT, Burg AB (1940) Metallo Borohydrides. I. Aluminum Borohydride. *J Am Chem Soc* 62: 3421–3425.
137.Schlesinger HI, Brown HC (1940) Metallo Borohydrides. III. Lithium Borohydride. *J Am Chem Soc* 62: 3429–3435.
138.Schlesinger HI, Brown HC, Hoekstra HR, et al. (1953) Reactions of Diborane with Alkali Metal Hydrides and Their Addition Compounds. New Syntheses of Borohydrides. Sodium and

Potassium Borohydrides1. *J Am Chem Soc* 75: 199–204.
139. Schlesinger HI, Brown HC, Abraham B, et al. (1953) New Developments in the Chemistry of Diborane and the Borohydrides. I. General Summary1. *J Am Chem Soc* 75: 186–190.
140. Miwa K, Aoki M, Noritake T, et al. (2006) Correlation between thermodynamic staibilties of metal borohydrides and cation electronegavities: First principles calculations and experiments. *Phys Rev B* 74: 075110.
141. Nakamori Y, Li H, Kikuchi K, et al. (2007) Thermodynamical stabilities of metal-borohydrides. *J Alloy Compd* 447: 296–300.
142. Hu J, Kwak JH, Zhenguo Y, et al. (2009) Direct observation of ion exchange in mechanism activated LiH+MgB2 system using ultrahigh field nuclear magnetic resonance spectroscopy. *Appl Phys Lett* 94: 141905.
143. Li H-W, Matsunaga T, Yan Y, et al. (2010) Nanostructure-induced hydrogenation of layered compound MgB2. *J Alloy Compd* 505: 654–656.
144. Pistidda C, Garroni S, Dolci F, et al. (2010) Synthesis of amorphous Mg(BH4)2 from MgB2 and H2 at room temperature. *J Alloy Compd* 508: 212–215.
145. Barkhordarian G, Jensen TR, Doppiu S, et al. (2008) Formation of Ca(BH4)2 from Hydrogenation of CaH2+MgB2 Composite. *J Phys Chem C* 112: 2743–2749.
146. Nwakwuo CC, Pistidda C, Dornheim M, et al. (2011) Microstructural analysis of hydrogen absorption in 2NaH+MgB2. *Scripta Materialia* 64: 351–354.
147. Garroni S, Minella CB, Pottmaier D, et al. (2013) Mechanochemical synthesis of NaBH4 starting from NaH–MgB2 reactive hydride composite system. *Int J Hydrogen Energy* 38: 2363–2369.
148. Nwakwuo CC, Hutchison JL, Sykes JM (2012) Hydrogen sorption in 3NaH+MgB2/2NaBH4+NaMgH3 composite. *Scripta Materialia* 66: 175–177.
149. Wang H, Zhang J, Liu JW, et al. (2013) Catalysis and hydrolysis properties of perovskite hydride NaMgH3. *J Alloy Compd* 580, Supplement 1: S197–S201.
150. Rafi ud d, Xuanhui Q, Zahid GH, et al. (2014) Improved hydrogen storage performances of MgH2–NaAlH4 system catalyzed by TiO2 nanoparticles. *J Alloy Compd* 604: 317–324.
151. Milošević S, Milanović I, Mamula BP, et al. (2013) Hydrogen desorption properties of MgH2 catalysed with NaNH2. *Int J Hydrogen Energy* 38: 12223–12229.
152. Li Y, Fang F, Song Y, et al. (2013) Hydrogen storage of a novel combined system of LiNH2-NaMgH3: synergistic effects of in situ formed alkali and alkaline-earth metal hydrides. *Dalton Transactions* 42: 1810–1819.